Trapping and Diffusion in the Surface Region of Cadmium Sulfide*

JAMES J. BROPHY
Physics Division, Armour Research Foundation, Chicago, Illinois
(Received February 19, 1960)

In lightly doped single crystal CdS illuminated with 4400 A radiation hole-electron pairs generated at the surface diffuse into the crystal until the hole is trapped. The electrons experience multiple retrapping until they disappear through recombination. Current noise and photoconductivity measurements are used to study these processes. The noise data establish the ambipolar diffusion length as 30 microns, confirm that diffusion is important though the appearance of a $f^{-\frac{3}{2}}$ trend in the noise spectra, and show that discrete traps are located the same distance below the conduction band in the surface regions as in the bulk. Discrete trap levels at 0.35, 0.40, and 0.43 volt below the conduction band are observed in the surface region. Trap densities of 10^{16} traps/cm^3 volt, an order of magnitude greater than that in the bulk, are determined. The trap frequency factors are of the order 10^{10} sec^{-1}.

I. INTRODUCTION

IN a previous paper,[1] hereafter referred to as I, we have demonstrated how current noise measurements coupled with photoconductivity data may be used to derive important information about the energy distribution and frequency factor of shallow traps in single crystal CdS. This work used 5200 A illumination which produces photoelectrons throughout the volume of the sample and therefore yields results characteristic of the bulk. In the present paper we extend the measurements to include 4400 A illumination which, because of the large absorption coefficient of CdS at this wavelength, generates carriers only at the surface and thus provides information about traps and trapping kinetics in the surface region.

Multiple trapping of photoelectrons in shallow traps causes fluctuations in the conduction band carrier density which may be observed as current noise. Noise measurements are capable of determining transition rates under steady-state conditions. By varying the illumination intensity the quasi Fermi level may be moved through the trap distribution and the contributions of the various trap levels evaluated. In I it was possible to derive trap escape probabilities from carrier fluctuation measurements and use this information to account satisfactorily for the observed noise spectra due to both discrete trap levels and those having a continuous distribution in energy.

Under 4400 A excitation electron-hole pairs produced in the surface region diffuse a short distance into the crystal by ambipolar diffusion before recombining. The trapping kinetics in this surface region, approximately one diffusion length deep, may be examined by the techniques used in I. The observed noise spectra furnish three important pieces of information in addition to trapping and retrapping rates: they confirm that diffusion occurs in that their shape is characteristic of diffusion noise; they establish that the discrete trap levels are located the same distance below the conduction band in the surface region as in the bulk; and they provide a measure of the ambipolar diffusion length. It proves possible to obtain good quantitative agreement between the observed noise characteristics and those predicted from trapping and diffusion processes.

II. EXPERIMENTAL TECHNIQUE

The same experimental technique as used in I was applied here with the 5200 A interference filter replaced by a 4400 A filter. The photoconductive time constant, τ_0, was determined oscillographically using a rotating glass chopper which produced a 4% change in intensity. At the lowest intensities it was necessary to use an opaque chopper to realize sufficient signal. The conduction band lifetime, τ_c, was calculated using $\tau_c=n_0/n_L$ where n_0 is the conduction band electron concentration determined from the conductivity and n_L is the electron generation rate due to photon absorption which is obtained from calibration of the light source with an Eppley thermopile and an assumed unity quantum efficiency.

Noise voltages appearing across a 1.25×10^4 ohm wirewound load resistor were measured with a standard tunable amplifier-voltmeter system and expressed as current fluctuations. A single 1.35-volt mercury cell supplied the current. The sample resistance was determined from the dc drop across the load resistor.

Two crystals taken from the same vapor phase growth batch, lightly CuCl doped during growth, were investigated. Sample dimensions were approximately 2.5 mm$\times$2.5 mm$\times$0.3 mm for both crystals. They were provided with low noise indium-soldered electrodes.

III. EXPERIMENTAL RESULTS

For comparison with the 4400 A illumination data, two noise spectra for these crystals taken at 5200 A which are similar to those found in I are shown in Fig. 1. The dashed lines in the figure represent slopes of -1, $-\frac{3}{2}$, and -2 and are included to facilitate comparison. These data, as discussed more fully in I, show a f^{-2} behavior at low frequencies with a turnover below 10 cps

* Supported by the Office of Naval Research.
[1] J. J. Brophy and R. J. Robinson, Phys. Rev. **117**, 738 (1960).

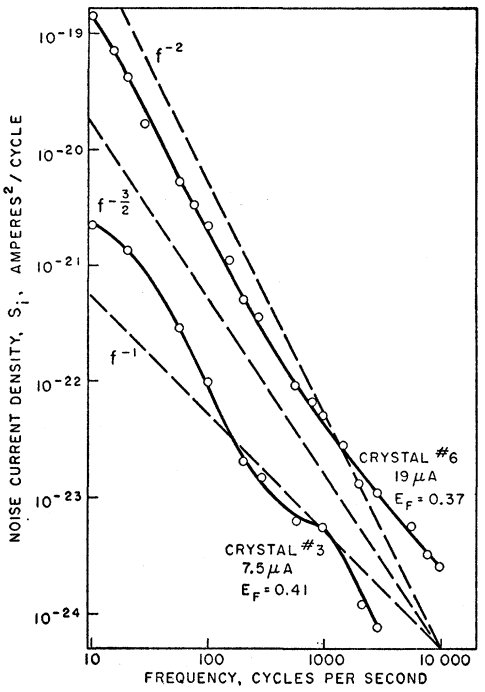

FIG. 1. Current noise spectra of crystals No. 3 and 6 under 5200 A illumination. The dashed lines, representing slopes of -1, $-\frac{3}{2}$, and -2, facilitate interpretation of the curves.

and a f^{-1} trend at high frequencies (crystal No. 6) or the appearance of a second relaxation frequency (crysta No. 3) at about 1100 cps when the quasi Fermi level is near 0.41 volt below the conduction band.

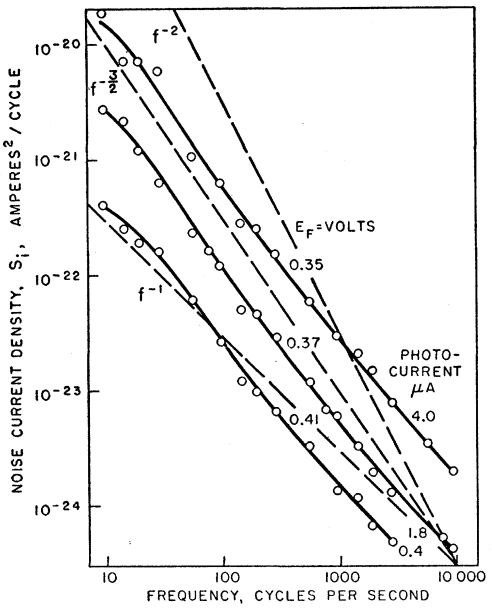

FIG. 2. Current noise spectra of crystal No. 6 under 4400 A illumination for three currents. The position of the quasi fermi level (E_F) for each curve is determined in Part III of the text.

Spectra under 4400 A illumination at three currents and for each crystal are shown in Figs. 2 and 3. In Fig. 2 (crystal No. 6) the spectra are clearly $f^{-\frac{3}{2}}$ at low frequencies and f^{-1} at high frequencies for all currents. The turnover frequency is again well below 10 cps. Similarly in Fig. 3 (crystal No. 3) a low-frequency turnover is followed by $f^{-\frac{3}{2}}$ behavior and two single relaxation frequencies at 1300 cps and 5000 cps for 0.51 and 2.4 microampere currents, respectively. Anticipating the discussion to follow below, we see that these spectra have either $1/f$ or discrete high-frequency relaxations which depend on trapping transitions and which are similar to those under 5200 A radiation. Similarly, a low-frequency turnover is common to all spectra. The

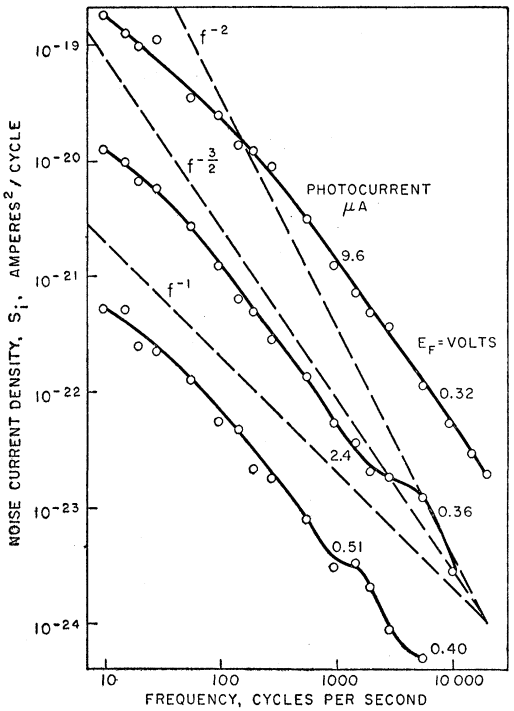

FIG. 3. Current noise spectra of crystal No. 3 under 4400 A illumination for three currents. The position of the quasi Fermi level (E_F) for each curve is determined in Part III of the text.

change from f^{-2} to $f^{-\frac{3}{2}}$ behavior will be shown to be due to diffusion of carriers into the crystal from where they are produced on the surface in the case of 4400 A illumination.

The photoconductive time constant, τ_0, and conduction band lifetime, τ_c, for both crystals and both wavelengths are shown as a function of current in Fig. 4. The data show that τ_0 is about the same at both wavelengths except at the higher currents, while τ_c is considerably smaller at 4400 A. The trends in τ_0 for crystal No. 3 are interesting in that the curves are similar except that the 4400 A data are displaced to lower currents.

Figure 5 shows the variation of low-frequency noise with current for both crystals and both wavelengths.

The data are presented in terms of carrier fluctuations, $\langle \Delta n^2 \rangle / n_0$, by the method used in I which will be discussed below. The peaks in the curves were shown in I to be due to trapping effects as the quasi Fermi level passes through the discrete trap levels. By comparing the position of the peaks for both wavelengths, we notice that the 4400 A curves appear displaced to lower currents by roughly an order of magnitude.

IV. INTERPRETATION

From published[2] optical absorption data, it is clear that the 4400 A photons are absorbed and produce electron-hole pairs in a depth of about 10^{-5} cm. These diffuse into the crystal until the holes are trapped. The electrons experience multiple trapping transitions until they disappear through recombination with the holes. During the multiple retrapping electrons cannot stray far from the region in which the holes have been trapped because of charge neutrality considerations. Thus, under 4400 A illumination the active region of the crystal is a thickness about equal to one ambipolar diffusion length.

TABLE I. Thickness of active surface layer.

Crystal	Method	Thickness—microns
3	Noise	31
	Noise	22
	Photoconductivity	20
6	Noise	30
	Noise	33
	Photoconductivity	22

If we assume for the moment that the discrete trap levels are the same distance below the conduction band in this surface region as in the bulk, an assumption that will be confirmed experimentally below, then corresponding peaks in Fig. 5 represent situations in which the quasi Fermi level is the same distance below the conduction band in the surface region as in the bulk. Under this condition the thickness of the surface region can be found from the ratio of the two currents and the crystal thickness since the entire crystal is active under 5200 A radiation. In the data of Fig. 5 there are two peaks for each sample which can be matched. These yield values of the order of 30 microns as shown in Table I. Also, the data of Fig. 4 determine trap density distributions after the manner derived in I and discussed below, and this purely photoconductive information can be used for a similar matching. The shape of the trap density distribution is independent of the thickness of the surface region. Matching the position of the discrete level peaks in the distributions yields the third entries in Table I. These six values compare very favorably with the ambipolar diffusion lengths recently reported[3]

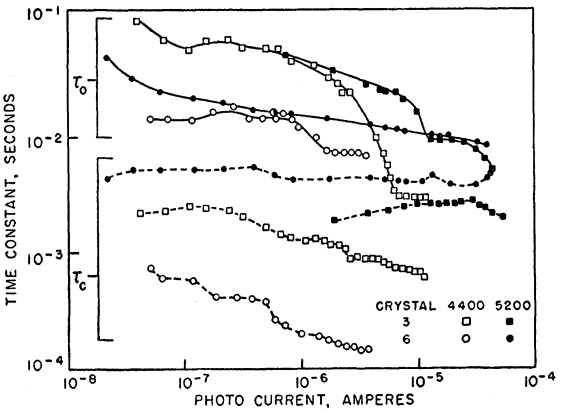

FIG. 4. Photoconductive time constants, τ_0, and conduction band lifetimes, τ_c, of both crystals as a function of current for 4400 A illumination (open data points) and 5200 A illumination (solid data points).

of 15 microns for unactivated crystals and 27 microns for silver activated crystals, using direct distance measuring techniques.

In order to confirm this picture, we turn to the noise spectra. The spectra of Fig. 1 can be understood from the analysis of I and previous work.[4,5] The spectra is made up of two components, a relaxation spectrum, $\tau_0/(1+\omega^2\tau_0^2)$, corresponding to electron recombination transitions which is characterized by the time constant τ_0 and which dominates at low frequencies, plus a relaxation spectrum characterized by a time constant related to trapping transitions and which is important at high frequencies. If the traps are distributed exponentially in energy, it is possible to generate a $1/f$ spectrum at high frequencies (see I). Discrete traps show up only when the quasi Fermi level is nearby be-

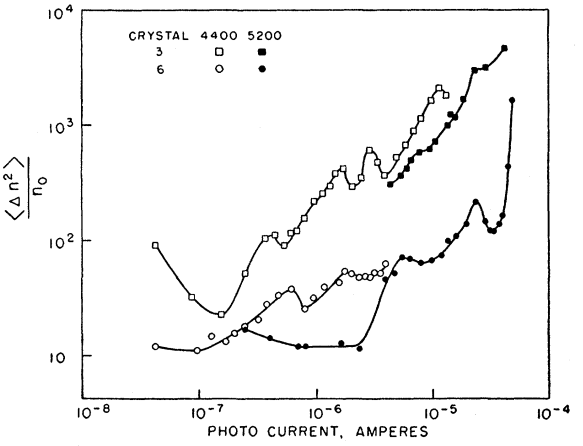

FIG. 5. Variation of the low-frequency noise, expressed in terms of carrier fluctuations, as a function of current for 4400 A illumination (open data points) and 5200 A illumination (solid data points).

[2] D. L. Dexter, J. Phys. Chem. Solids 8, 473 (1959).
[3] J. Auth and R. Ridder, Ann. Physik 2, 351 (1959).
[4] K. M. Van Vliet et al., Physica 22, 723 (1956).
[5] K. M. Van Vliet and J. Blok, Physica 22, 525 (1956).

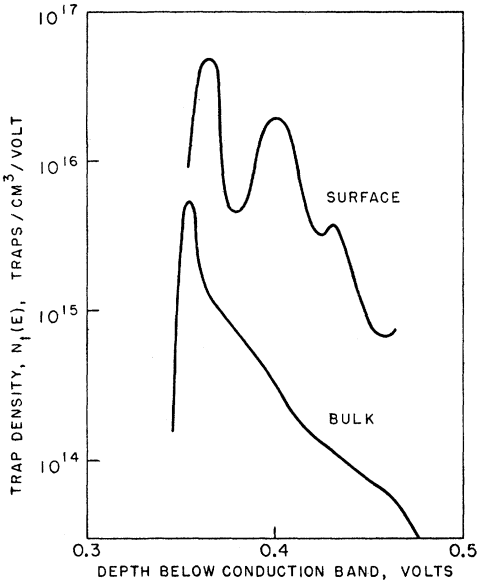

FIG. 6. Energy distribution of traps in the bulk and in the surface region for crystal No. 6.

cause of occupancy considerations and they then yield a high-frequency relaxation "bump" in the spectra. Both high-frequency behaviors are shown in Fig. 1 for the two crystals. In particular, crystal No. 3 shows the presence of a discrete trap with a relaxation frequency of 1100 cps located 0.41 volt below the conduction band.

In Fig. 3 we again see evidence for a discrete trap with a relaxation frequency of 1300 cps at a photocurrent of 0.51 microampere. Using the thickness given in Table I this current corresponds to a quasi Fermi level position in the surface region of 0.40 volt below the conduction band, in excellent agreement with Fig. 1. Since the time constant associated with this trap depends on its depth below the conduction band, these data clearly establish that the trap depth in the surface region is the same as that in the bulk. In Fig. 3 another relaxation phenomenon at 5000 cps is evident at 2.4 microamperes. This current corresponds to a depth of 0.36 volt, again in good agreement with the known position of a discrete level (compare I and Fig. 7, below). Finally, the ratio of frequencies of these two discrete levels should depend exponentially on the difference in their energy depths. We find that $5000/1300=3.8 \approx \exp(0.4-0.36)38.6=4.7$, which in good agreement considering that the particular currents chosen may not have put the quasi Fermi level exactly at the trap depth.

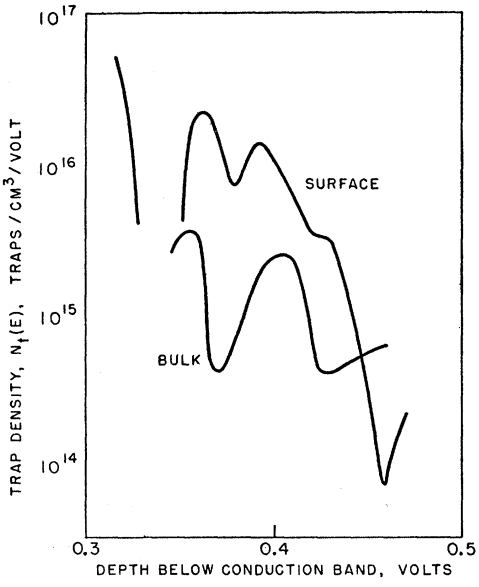

FIG. 7. Energy distribution of traps in the bulk and in the surface region for crystal No. 3.

The $f^{-\frac{3}{2}}$ behavior of the spectra at 4400 A is evidence for diffusion noise,[6] which is additional confirmation of the picture presented. The diffusion noise phenomenon is discussed quantitatively in Part VI.

On the basis of this information we believe the picture presented above is correct and that the noise and photoconductive measurements at 4400 A are characteristic of a region 30 microns thick on the surface. Since this distance is considerably greater than the thickness of any presumed semiconductor surface barrier region, it is perhaps not surprising that, for example, the trap depth is the same here as throughout the bulk. However, as shown below, the trap density and frequency factors are different here than in the volume.

V. TRAP CHARACTERISTICS

The techniques used to determine the trap distribution in energy and the trap frequency factors as derived in I may be directly applied here. The pertinent relations used are summarized in Table II for convenience. A surface region thickness of 25 microns was assumed for these calculations.

The trap energy distribution is calculated from the photoconductivity data alone, as shown in Table II, using the data of Fig. 4. The results are shown in Figs. 6 and 7 for crystals No. 6 and No. 3, respectively. The

TABLE II. Summary of equations.

Trapped electron concentration,	$h_0=n_0(\tau_0-\tau_c)/\tau_c$
Carrier fluctuations,	$\langle\Delta n^2\rangle/n_0=(m+1)$
Trap energy density,	$N_t(E_F)=dh_0/dE_F$
Trap frequency factor,	$S(E_F)=(N_c/N_t)[(m/\tau_c)/kT+d(m/\tau_c)/dE_F]$

where

n_0 = conduction band carrier density
τ_0 = photoconductive decay constant
τ_c = conduction band lifetime
m = average number of times trapped
E_F = quasi Fermi level position above valence band
N_c = conduction band state density

[6] M. Lax and P. Mengert, Second Conference on Semiconductor Surfaces, Naval Ordnance Laboratory, December, 1959 (unpublished).

trap densities in the surface region are about an order of magnitude larger than those in the bulk, but there are other features in common. All curves show the presence of a strong level near 0.36 volt and crystal No. 3 also has a level at 0.40 volt which appears in both the surface and bulk. Crystal No. 6 has this level on the surface but only a slight suggestion of it in the bulk. Both crystals seem to have an additional discrete level at 0.43 volt on the surface which is not evident in the bulk. Thus, there is considerable correlation between the trap concentrations in the bulk and on the surface, as well as significant differences.

Calculation of the trap frequency factor brings in the noise data through the average number of times trapped, m, which is determined from the carrier fluctuations. It should be emphasized here again that these data are derived from low-frequency noise measurements alone. The current noise density, S_i, on the low-frequency plateau determines m. The frequency factors for the crystals are shown in Fig. 8. The frequency factors are smaller in the surface region than in the bulk. However, here again similarities exist in structure of the curves. While there can be some question as to the reliability of such structure since the calculated frequency factors are the result of two graphical differentiations, the consistency with which the structure appears in the data appears to be significant. Each peak in the $S(E)$ curve corresponds to a discrete trap level.

With regard to the magnitude of $S(E)$, these values are larger than those derived from thermally simulated current measurements,[7] but appear to be in agreement with those obtained from photoconductivity experiments.[8] In comparing the present surface and bulk values, it should be noted that $S(E)$ involves division by N_t. Thus, if the N_t values for the bulk were small for any reason the $S(E)$ would be large. In computing the bulk values, it is assumed that the traps are uniformly distributed throughout the volume. If the traps were concentrated in the surface regions, a low value for N_t would result (see Figs. 6 and 7). Thus these results may suggest that the traps are predominantly in the surface regions.

TABLE III. Frequency at which trapping noise appears (crystal No. 6).

	Position of quasi Fermi level below conduction band—volts		
	0.351	0.374	0.411
τ_0	6.5×10^{-3} sec	7.3×10^{-3} sec	1.5×10^{-2} sec
τ_c	1.4×10^{-4} sec	1.8×10^{-4} sec	4.0×10^{-4} sec
$m+1$	60	45	27
$\hat{n}'$	8.6×10^{14} cm^{-3}	3.1×10^{14} cm^{-3}	7×10^{13} cm^{-3}
n_0	3.9×10^{13} cm^{-3}	1.6×10^{13} cm^{-3}	3.9×10^{12} cm^{-3}
$\nu=m/\tau_c$	4.3×10^{5} sec^{-1}	2.5×10^{5} sec^{-1}	6.7×10^{4} sec^{-1}
$g'=m/(\tau_0-\tau_c)$	9.4×10^{3} sec^{-1}	6.3×10^{3} sec^{-1}	1.8×10^{3} sec^{-1}
f_a (calculated)	890 cps	590 cps	200 cps
f_a (experimental)	800 cps	550 cps	200 cps

[7] R. H. Bube, J. Chem. Phys. **23**, 18 (1955).
[8] K. W. Boer and H. Wantosch, Ann. Physik **2**, 406 (1959).

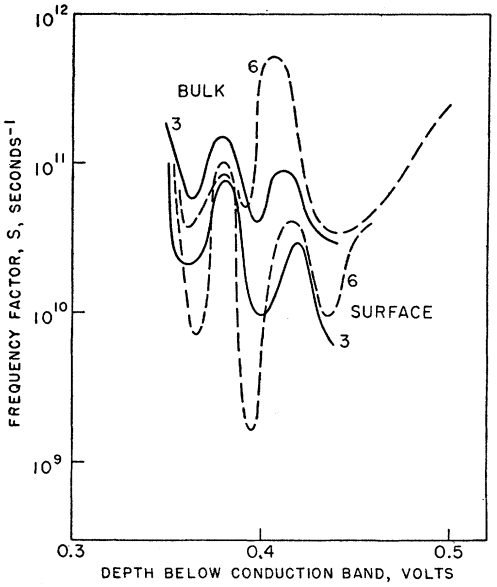

FIG. 8. Frequency factor of traps in the bulk and in the surface region for crystals Nos. 3 and 6.

VI. DIFFUSION NOISE

The $f^{-\frac{3}{2}}$ behavior of noise spectra dominated by diffusion effects has been predicted,[6] together with the remark that the diffusion contribution is difficult to observe in the absence of trapping. We have already noted how the diffusion noise characteristics of the spectra confirm the picture of processes in the surface region in the case of CdS. Furthermore, the data independently show the presence of multiple trapping, as required.

According to Lax[6] the frequency at which the retrapping noise should start to contribute (thus the high-frequency limit to the $f^{-\frac{3}{2}}$ behavior) is given by

$$\omega_a=[(D\nu)^{\frac{1}{2}}\nu_a\hat{n}'/nL]^{\frac{1}{2}},$$

where D is the diffusivity, ν is the trapping rate, ν_a is a parameter involving ν and the trap release rate, $\hat{n}'$ is a parameter related to the trapped electron concentration, n is the carrier density, and L is the distance between electrodes. This expression is evaluated in Table III for conditions pertaining to crystal No. 6 under which the spectra of Fig. 2 were measured.

Using Fig. 2, experimental values for the frequency at which $1/f$ noise begins were obtained from the intersection of the extrapolated $f^{-\frac{3}{2}}$ trend to the extrapolated f^{-1} trend. Comparison of the last two lines of Table III shows very satisfactory agreement between predicted and observed values.

We must also be concerned with the low-frequency limit of the $f^{-\frac{3}{2}}$ behavior to be sure that diffusion noise does not interfere with calculation of carrier density

fluctuations from low-frequency noise measurements. The frequency of the lower limit of the $\frac{3}{2}$ power law is given by Lax as $2L^2/\tau_0^2 D$ which, using the data of Table III results in values of 80, 70 and 17 cps. These are sufficiently far above the lower turnover frequency due to τ_0 to justify the procedure. Unfortunately, the experimental data are not sufficiently extensive in this region to allow an experimental estimate of these frequencies for comparison. However, the spectra are not inconsistent with these values.

VII. ACKNOWLEDGMENT

The author has benefited considerably by the opportunity to discuss much of this work with Robert J. Robinson whose continued enthusiasm is sincerely appreciated.

PHYSICAL REVIEW VOLUME 119, NUMBER 2 JULY 15, 1960

Linear Antiferromagnetic Chain*

T. W. RUIJGROK†
Department of Physics, University of Washington, Seattle, Washington

AND

S. RODRIGUEZ
Department of Physics, University of Illinois, Urbana, Illinois

(Received February 16, 1960)

The properties of the low-lying states of the antiferromagnetic chain are studies by means of a variational method. A trial wave function is exhibited which has an energy very close to that of the correct ground state and which displays a long-range order.

I. INTRODUCTION

WE are concerned, in the present work, with a system of N atoms of spin $\frac{1}{2}$ arranged on a line and coupled together by an interaction described by the Hamiltonian operator

$$H=\tfrac{1}{2}J\sum_j(\boldsymbol{\sigma}_j\cdot\boldsymbol{\sigma}_{j+1}-1). \tag{1}$$

The quantity J is the exchange integral and is positive for an antiferromagnetic lattice. The operator $\boldsymbol{\sigma}_j$ is the Pauli spin operator associated with the jth atom in the line. The sum over j extends over all the atoms in the system.

Several authors[1–4] have examined this problem by a method that consists in writing the Hamiltonian (1) in terms of anticommuting operators. The expression (1) can be written in the form

$$H=H_0+H_1, \tag{2}$$

where

$$H_0=\sum_k \epsilon(k)\eta^*(k)\eta(k), \tag{3}$$

and

$$H_1=2JN^{-1}\sum_{k_1k_2k_3k_4} v(k_1k_2k_3k_4)\eta^*(k_1)\eta(k_2)\eta^*(k_3)\eta(k_4), \tag{4}$$

with

$$\epsilon(k)=-2J(1-\cos k), \tag{5}$$

and

$$v(k_1k_2k_3k_4)=\exp[i(k_1-k_2)]\bar{\Delta}(k_1-k_2+k_3-k_4). \tag{6}$$

The wave number k takes the values $2\pi n/N$, in which n is an integer and where two wave numbers k and k' differing by an integral multiple of 2π are to be considered identical. The symbol $\bar{\Delta}(k)$ is unity when k is zero or an integral multiple of 2π, and zero otherwise. The operators $\eta^*(k)$ and $\eta(k)$ satisfy the anticommutation relations characteristic of operators representing the creation and destruction of Fermi particles, i.e., we have

$$\{\eta^*(k),\eta^*(k')\}=\{\eta(k),\eta(k')\}=0, \tag{7}$$

and

$$\{\eta^*(k),\eta(k')\}=\bar{\Delta}(k-k'). \tag{8}$$

The operator (2) has been discussed in more detail elsewhere.[4] It will be sufficient here to remark that, as the ground state is a singlet,[5] we need only consider states in which there are $N/2$ Fermi particles present. This is immediately understood by looking at the identity

$$\sum_k \eta^*(k)\eta(k)=\tfrac{1}{2}N+\tfrac{1}{2}\sum_j \sigma_j^{(z)}. \tag{9}$$

The ground-state energy of (1) has been calculated exactly by Hulthén[6] using a method invented by Bethe.[7] Approximations to the ground-state wave function, using the variational principle have been given by

* Supported in part by the U. S. Atomic Energy Commission.
† On leave of absence from the Rijksuniversiteit, Utrecht, The Netherlands.
[1] Y. Nambu, Progr. Theoret. Phys. (Kyoto) **5**, 1 (1950).
[2] I. Syozi, Busseiron-Kenkyu **39**, 55 (1951).
[3] K. Meyer, Z. Naturforsh. **11a**, 865 (1956).
[4] S. Rodriguez, Phys. Rev. **116**, 1474 (1959).
[5] W. Marshall, Proc. Roy. Soc. (London) **A232**, 48 (1955).
[6] L. Hulthén, Arkiv Mat. Astron. Fysik **26A**, No. 1 (1938).
[7] H. A. Bethe, Z. Physik **71**, 205 (1931).